Visual Acuity Is Reduced in Alpha 7 Nicotinic Receptor Knockout Mice

Nicola Origlia,[1] *Dario Riccardo Valenzano,*[2] *Milena Moretti,*[3] *Cecilia Gotti,*[3] *and Luciano Domenici*[1,4]

Purpose. Nicotinic receptors (nAChRs) are part of a heterogeneous family of pentameric ligand-gated ion channels that are widely expressed in the visual system. The impact of $\alpha 7$ homomeric nAChRs on visual function was investigated using mutant mice lacking the $\alpha 7$ nicotinic receptor subunit.

Methods. The spatial resolution limit was measured in $\alpha 7$ knockout ($\alpha 7$ KO) and age-matched control mice using three independent methods: an operant behavioral visual task (Prusky maze), cortical visual evoked potentials (VEPs), and the pattern electroretinogram (PERG) evoked by alternating gratings of different spatial frequencies and contrasts.

Results. Visual acuity measured by means of the visual water maze task was significantly decreased in the $\alpha 7$ KO mice and, concordantly, there was a reduction of the cortical spatial resolution limit measured by VEPs. However, the PERG was normal in $\alpha 7$ KO mice, compared with control mice. The use of fluorescently tagged cholera toxin showed that projections from the retina segregate normally in $\alpha 7$ KO mice and, in line with this, the visual cortical responses elicited by stimulating either eye were normally balanced in both visual cortices and showed no retinotopic anomalies.

Conclusions. These findings indicate that the absence of the $\alpha 7$ nicotinic subunit reduces visual acuity. Because the cortical output has an abnormal spatial resolution but retinal output is preserved, it can be concluded that the low visual acuity was due to a deficit specifically present in the visual cortex. (*Invest Ophthalmol Vis Sci.* 2012;53:1211–1218) DOI:10.1167/iovs.11-8007

Nicotinic receptors (nAChRs) represent a heterogeneous family of ion channels that are differently expressed in the nervous system. There are 12 subunit genes that derive from a common ancestral gene: 9 α subunits ($\alpha 2$ to $\alpha 10$) and 4 β subunits ($\beta 2$ to $\beta 4$). Neuronal nAChRs fall into two main classes: homomeric or heteromeric α-bungarotoxin (αBgtx)–sensitive receptors consisting of $\alpha 7$, $\alpha 8$, or $\alpha 7$–$\alpha 8$ and/or $\alpha 10$ subunits and αBgtx-insensitive heteromeric receptors consisting of $\alpha 2$–$\alpha 6$ and $\beta 2$–$\beta 4$ subunits. Nicotinic AChRs are permeable to Na^+, K^+, and Ca^{2+} ions, and their cation permeability is influenced by their subunit composition. The $\alpha 7$ subunit that forms native pentameric homomeric receptors is highly expressed in the hippocampus, hypothalamus, and neocortex of rodents.[1] Alpha-7 knockout (KO) mice, which are characterized by the loss of αBgtx receptors and the lack of nicotine-evoked fast desensitizing currents in neurons,[2] are viable with apparently normal brain anatomy.

In terms of behavior, the performance of $\alpha 7$ KO mice in the classic Morris water maze test, the Pavlovian conditioned fear test and the prepulse inhibition paradigm are similar to those of wild-type (WT) mice, which suggests that the absence of $\alpha 7$ nAChRs has little impact on normal, baseline behavioral responses.[3] Moreover, $\alpha 7$ KO mice show a reduced anxiety-related response,[3] whereas only mice lacking both the $\alpha 7$ and the $\beta 2$ nAChR subunits show impaired learning and memory in a passive avoidance test, and enhanced motor activity on the rota rod.[4] More recently, a deficit in a modified Morris water maze task (delayed matching to place preference) has been described in mice lacking the $\alpha 7$ subunit,[5] thus suggesting a minor impairment in episodic/working memory such as that observed in previous hippocampus studies based on the infusion of an $\alpha 7$ subunit antagonist.[6]

Although $\alpha 7$ KO mice are widely used in behavioral studies, no attempt has been made to characterize their visual function. The $\alpha 7$ subunit is widely expressed in the visual system, particularly in the retina and retinal input recipient regions such as the dorsolateral geniculate nucleus (dLGN), the superior colliculus, and the visual cortex.[1,7,8] Recent studies have shown that visual system development and function require the activity of nAChRs: in particular, the $\beta 2$ subunit is required for the formation of eye-specific layers at the thalamic level, a process that depends on retinal waves of spontaneous activity.[9,10] However, the impact of a complete lack of the $\alpha 7$ nicotinic subunit on visual system development and functional phenotype acquisition is still unknown.

Methods

Animals

All the experiments were carried out in accordance with the European Community Council Directive concerning the treatment of animals using mice at least 2 months old. We used $\alpha 7$ KO mice homozygous for the *Chrna7*^{tm1Bay} mutation (Jackson Laboratory, Bar Harbor, ME) and, in parallel, mice of the same mixed genetic background (C57BL/6J) as controls. To exclude the possibility that the mixed genetic background of the mutant mice may affect the results of the study, the $\alpha 7$ KO mice were backcrossed for 10 generations onto the C57BL/6 strain (Jackson Laboratory).

Binding Assay and Immunoprecipitation

The sequences of polyclonal antibodies against the $\alpha 2$, $\alpha 3$, $\alpha 4$, $\alpha 5$, $\alpha 6$, $\beta 2$, $\beta 3$, and $\beta 4$ peptides were raised and characterized as previously

From the [1]Neuroscience Institute (National Council of Research [CNR]), Pisa, Italy; the [2]Department of Genetics, Stanford University, Stanford, California; the [3]CNR Neuroscience Institute, Cellular and Molecular Pharmacology, Department of Medical Pharmacology, University of Milan, Milan, Italy; and the [4]Department of Technological and Biomedical Sciences, University of L'Aquila, L'Aquila, Italy.

Supported in part by a European Council Grant 202088 Neurocypres and an Interuniversity Research Program for the Development of Research of National Interest Grant PRIN 2009R7WCZS (CG).

Submitted for publication June 7, 2011; revised December 19, 2011, and January 19, 2012; accepted January 19, 2012.

Disclosure: **N. Origlia**, None; **D.R. Valenzano**, None; **M. Moretti**, None; **C. Gotti**, None; **L. Domenici**, None

Corresponding author: Luciano Domenici, Neuroscience Institute (C.N.R.), Via G. Moruzzi 1, 56100, Pisa, Italy; domenici@in.cnr.it.

described.[11] We used antibodies directed only against peptides located in the cytoplasmic loop between M3 and M4 (CYT) of the $\alpha 2$, $\alpha 3$, $\alpha 4$, $\alpha 5$, $\alpha 6$, $\beta 2$, $\beta 3$, and $\beta 4$ subunits. The specificity and immunoprecipitation capacity of most of the antibodies have been previously described.[11,12]

The eyes and visual cortex were dissected, immediately frozen in liquid nitrogen, and then stored at −80°C for later use. In each experiment, the eyes or visual cortex were separately homogenized in an excess of 50 mM Na phosphate (pH 7.4), 1 M NaCl, 2 mM EDTA, 2 mM EGTA, and 2 mM phenylmethylsulfonylfluoride (PMSF) for 2 minutes in a commercial homogenizer (Ultra Turrax; IKA Works, Wilmington, NC), after which the homogenates were diluted and centrifuged for 1.5 hours at 60,000*g*. The whole eyes and visual cortex were homogenized, diluted, and centrifuged twice, after which the pellets were collected, rapidly rinsed with 50 mM Tris-HCl (pH 7), 120 mM NaCl, 5 mM KCl, 1 mM $MgCl_2$, 2.5 mM $CaCl_2$, and 2 mM PMSF, and then resuspended in the same buffer containing a mixture of 10 μg/mL of each of the following protease inhibitors: leupeptin, bestatin, pepstatin A, and aprotinin. Triton X-100 at a final concentration of 2% was added to the washed membranes, which were extracted for 2 hours at 4°C. The tissue extracts were then centrifuged for 1.5 hours at 60,000*g*, recovered, and an aliquot of the resultant supernatants was collected for protein measurement using the BCA protein assay (Pierce Protein Research Products, Thermo Fisher Scientific, Rockford, IL) with bovine serum albumin as the standard.

The specific activity of the [^{125}I]α-Bgtx (PerkinElmer, Boston, MA) was 150 Ci/mmol. Binding to the visual cortex membranes was performed by means of overnight incubation with a saturating concentration of 5 nM [^{125}I]α-Bgtx at room temperature. Nonspecific binding was determined in parallel by means of incubation in the presence of 1 μM unlabeled α-Bgtx. After incubation, the samples were filtered and the bound radioactivity was directly counted in a γ counter. To ensure that the $\alpha 7$ subtype did not contribute to ^{3}H-epibatidine (^{3}H-Epi) binding, the binding to the Triton X-100 extracts and the immunoprecipitation experiments were performed in the presence of 1 μM αBgtx, which specifically binds to the $\alpha 7$ subtype and prevents Epi from binding to the subtypes containing this subunit. The binding to the tissue extracts was performed by incubating the extracts with 2 nM ^{3}H-Epi in the presence and absence of 100 nM cold Epi using an ion-exchange resin (DE52; Whatman, Maidstone, UK) as previously described.[11,12]

For the immunoprecipitation experiments, the extracts obtained from tissues preincubated with 1 μM αBgtx were labeled with 2 nM ^{3}H-Epi and then incubated overnight with a saturating concentration of affinity-purified anti–subunit-specific IgG (20 μg). The immunoprecipitation was recovered by incubating samples with beads containing bound anti-rabbit goat IgG (Technogenetics, Milan, Italy). The level of antibody immunoprecipitation was expressed as fmol of immunoprecipitated receptors/mg of protein.

Behavioral Assessment of Visual Acuity Using the Visual Water Task

A behavioral measure of visual acuity was obtained using the method described by Prusky et al.[13] Starting at postnatal day 60 (P60), the $\alpha 7$ KO ($n = 5$) and WT mice ($n = 5$) were trained and tested in the visual water task for 10 trials every day to assess their visual acuity. The visual water task first trains the animals to choose a low (0.05 cycle/deg) spatial frequency vertical grating from gray and then tests the limit of their discrimination ability at increasing spatial frequencies. The highest spatial frequency at which 70% discrimination accuracy is achieved is taken as the visual acuity. (See Fig. 2A later in text, which shows a schematic representation of the visual water task.)

VEP and ERG Recordings

Visual evoked potentials were recorded as described by Porciatti et al.[14] Briefly, the mice were anesthetized by means of an intraperitoneal injection of 20% urethane and mounted in a stereotactic apparatus allowing a full view of the visual stimulus. After carefully removing a portion of the skull overlying the binocular visual cortex while leaving the dura intact, a glass-pulled recording electrode filled with NaCl (3 M) was inserted into the cortex perpendicularly to the stereotaxic plane. The electrical signals were amplified (10,000-fold), band-pass filtered (0.3–100 Hz), digitized, and averaged (at least 75 events in blocks of five events each). The transient VEPs in response to an abrupt contrast reversal (1 Hz) were evaluated in the time domain by measuring the peak-to-trough amplitude and peak latency of the major component. The visual stimuli consisted of horizontal gratings of different spatial frequencies and contrasts generated by a visual stimulator interface (VSG2:2 card; Cambridge Research System, Cheshire, UK) and presented on the screen of a monitor (Sony model CPD-G520) placed 20 cm in front of the animal. To obtain an estimate of contralateral ocular bias using VEPs, the electrode was positioned 2.8–3 mm laterally to lambda in accordance with the retinotopy and ocularity analysis described by Porciatti et al.[14]; in agreement with these previous data, the response to a windowed stimulus with different azimuths gave a maximal amplitude at nearly 10° lateral to the vertical midline.

The flash ERG (F-ERG) was evoked by means of 10-ms flashes of light generated by a commercial optical stimulator (Ganzfeld stimulator; Lace, Pisa, Italy). The electrophysiological signals were recorded through gold-plate electrodes inserted under the lower eyelids and in contact with the cornea, which had been previously anesthetized with ossibuprocaine (Novesine; Novartis Pharma, Basel, Switzerland). The corneal electrode at each eye was referred to a needle electrode (one on each side) subcutaneously inserted into the ipsilateral region behind the ear. The different electrodes were connected to a two-channel amplifier.

For the recordings made under scotopic conditions, the animals were dark adapted (300 minutes), anesthetized with an intraperitoneal injection of 2,2,2-tribromoethanol (Avertin 2 mL/100 g body wt; 1.25% [w/v] 2,2,2-tribromoethanol; and 2.5% [w/v] 2-methyl-2-butanol; Sigma–Aldrich, St. Louis, MO), and loosely mounted in a stereotaxic apparatus under dim red light. Their body temperature was kept at 37.5°C and their heart rate was monitored. Immediately before the recording session, the pupil was dilated by topically applying one eye drop containing atropine (0.5% sol; Allergan, Pomezia, Italy). The scotopic ERGs were recorded in response to single flashes of different light intensities ranging from 10^{-4} to 20 cd/m^2 $\times$ s^{-1}. The photopic ERGs were obtained using a single flash of 20 cd s/m^2 $\times$ s^{-1} in the presence of constant background illumination of 15 cd/m^2. The b-wave amplitude of each eye was averaged and plotted as a function of increasing luminance (transfer curve); for each animal group, the mean b-wave amplitude was plotted as a function of different luminances and rearing conditions.

The pattern electroretinograms (PERGs) were recorded as described in Porciatti et al.[15,16] using a recording electrode made of a thin silver wire (diameter, 0.25 mm) configured as a semicircular loop, with a radius of 2 mm, that was gently placed on the corneal surface by means of a micromanipulator under microscopic control. To maximize the PERG amplitude, patterned visual stimuli were used as described earlier at a mean luminance of 30 cd/m^2, with different spatial frequencies and contrasts.

Fluorescent Tracing of Retinogeniculate Projections

Adult mice were anesthetized with 2,2,2-tribromoethanol (Avertin 2 mL/100 g body wt) and 2 μL of 1% Alexa Fluor 488–conjugated (Invitrogen) cholera toxin B (CTB) subunit was injected into one eye using pulled glass capillaries inserted just behind the corneoscleral margin. After 48 hours, the mice were anesthetized and perfused with 4% paraformaldehyde in PBS. Their cryoprotected brains were cut into 40-μm coronal sections using a freezing microtome. The images of the sections were acquired using an optical microscope (Nikon) and analyzed using ImageJ software (developed by Wayne Rasband, National Institutes of Health, Bethesda, MD; available at http://rsb.info.nih.gov/

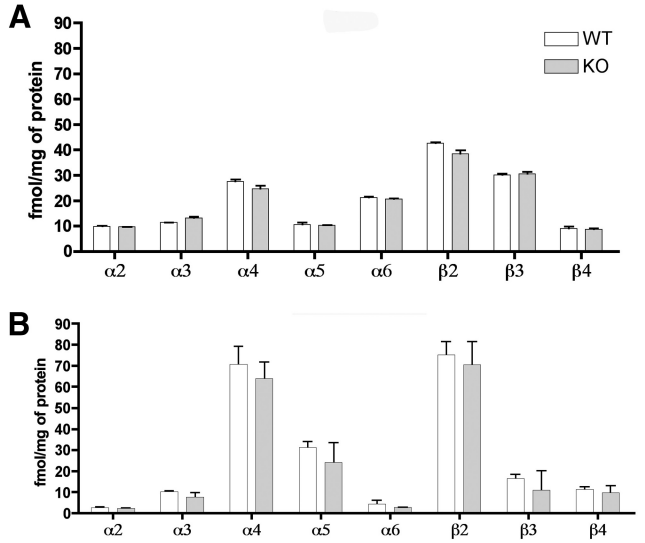

FIGURE 1. Immunoprecipitation analysis of the subunit content of the ^{3}H-Epi receptors expressed in retina and visual cortex. Triton X-100 (2%) extracts were obtained from membranes prepared from eyes and visual cortex preincubated with 2 μM αBgtx, and then labeled with 2 nM ^{3}H-Epi. Immunoprecipitation was carried out using saturating concentrations (20 μg) of antisubunit antibodies. In each experiment, the amount immunoprecipitated by each antibody was subtracted from the value obtained in control samples containing an identical concentration of normal rabbit IgG. The results for retina (**A**) and visual cortex (**B**) are expressed as fmol of labeled ^{3}H-Epi receptor/mg of protein, and represent the mean values ± SEM of two (eyes) and three experiments performed in duplicate.

ij/index.html). The limits of the ipsilateral and contralateral dLGN projections were traced on the computer screen, and the percentage dLGN area occupied by ipsilateral fibers was calculated by dividing the average of the ipsilateral areas (corresponding to the middle third of the dLGN) by the average of the total dLGN areas.

Statistics

Student's *t*-test was used to compare the data obtained from the α7 KO and WT mice. A value of $P < 0.05$ was considered statistically significant.

RESULTS

The α7 KO mice were anatomically and morphologically indistinguishable from the mice of the same mixed genetic background (C57BL/6J mice) used as controls.

Although the findings of a considerable number of studies of α7 KO mice have been published, little is known about the developmental changes in nAChR subunits occurring in the brains of α7-deficient mice. We investigated the levels of different nAChR subunits in the retina and cortex of α7 KO and WT mice, and analyzed the presence of α7-containing receptors by means of binding with the specific α7 ligand, ^{125}Iα-Bgtx. As expected, specific binding of ^{125}Iα-Bgtx was observed only in the visual cortex of the WT but not in α7 KO mice (17.8 ± 1.3 vs. 0.3 ± 0.1 fmol of specifically bound ^{125}Iα-Bgtx/mg of protein). The expression pattern of heteromeric receptors in the retina and visual cortex of the WT and α7 KO mice was very similar (Fig. 1), with no statistical differences in the levels of receptors containing the α2, α3, α4, α5, α6, β2, β3, and β4 subunits. Our findings in mouse retina are in line with those previously determined in rat[17] and exclude the possibility that the expression of non-α7 nicotinic subunits is altered in α7 KO mice.

Because previous studies of α7 KO mice have found minor alterations in the learning of spatial tasks, we used the visual water task developed by Prusky et al.[13] to generate a behavior-based measure of visual acuity (Fig. 2). The test involves learning an associating task in a visual water maze (see schematic drawing in Fig. 2A). The behavioral visual acuity of the WT controls was in line with previous findings,[13] and there was no difference in learning ability between the control and α7 KO mice: 90% of correct choices was achieved in 10 sessions by both groups. However, visual acuity was significantly reduced in the α7 KO mice (0.38 ± 0.01 cycle/deg, $n = 5$, vs. 0.51 ± 0.02 cycle/deg, $n = 5$; $P < 0.05$).

VEP recordings were used to relate behaviorally assessed visual acuity to cortical electrophysiological responses to patterned visual stimuli. The VEPs were recorded in at least three spaced positions in the binocular portion of the primary visual cortex.[14] At low spatial frequencies (0.06–0.1 cycle/deg, contrast = 90%), the VEPs consisted of a major negative component with a mean latency of 108 ± 5 ms in WT and 104 ± 4 ms in α7 KO mice ($P > 0.05$; typical examples are shown in Fig. 3A). Spatial frequencies of <0.06 cycle/deg were not used because it was technically impossible to include a sufficient number of cycles (at least three) on our computer screen. In the control mice, VEP amplitudes decreased at spatial frequencies of >0.06 cycle/deg until the signal became indistinguishable from the noise level (calculated for 0% contrast; see Fig. 3A). The

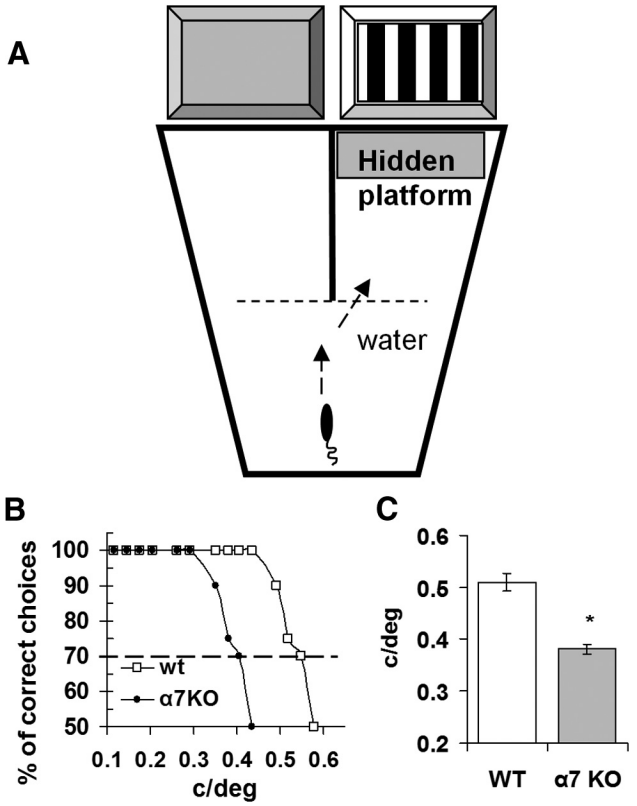

FIGURE 2. (**A**) Schematic representation of the visual water task. The mice are released in the long arm of the water maze and trained to reach a submerged "hidden platform" associated with the compartment displaying the low-frequency grating, which is positioned in either arm of the maze in a pseudorandom sequence. Once a mouse reaches a 90% success rate in choosing the arm of the maze showing the grating, the grating's spatial frequency is progressively increased until its discrimination rate drops to 70%. This value is used as a measure of actual visual acuity. (**B**) Examples of acuity assessment. (**C**) Mean visual acuity was significantly decreased in the adult α7 KO mice (0.38 ± 0.01 vs. 0.51 ± 0.02 cycle/deg; $n = 5$; $^{*}P < 0.05$).

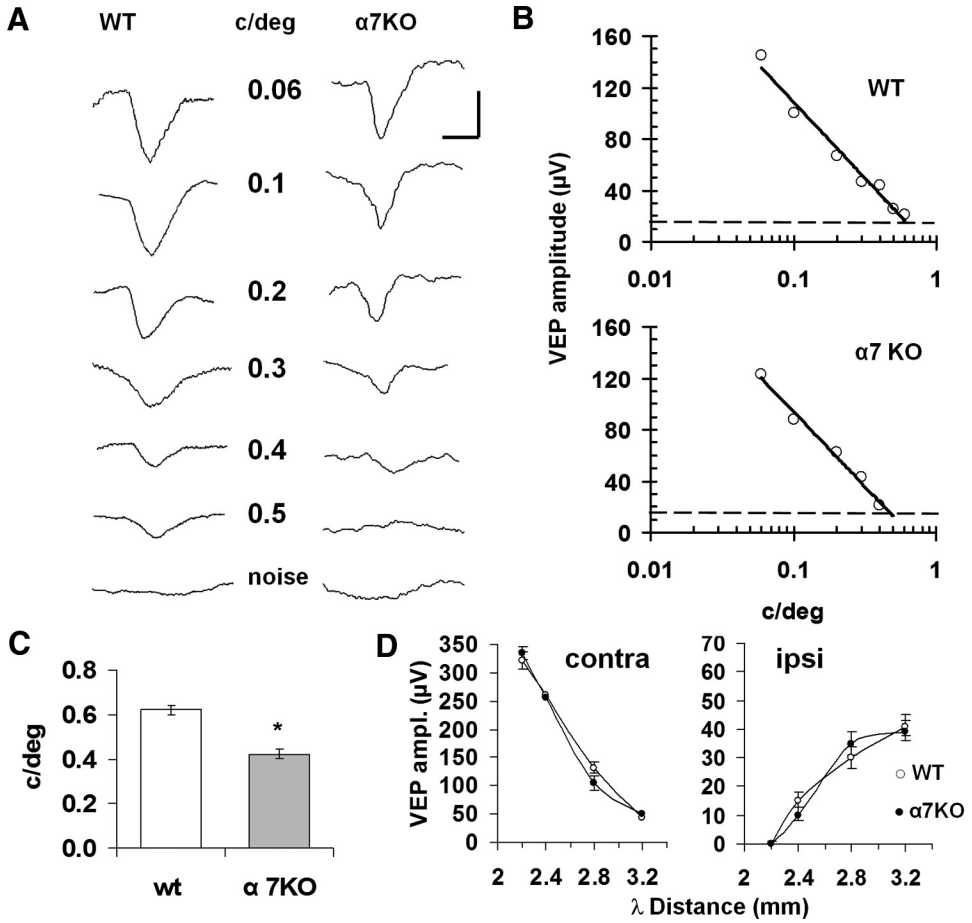

FIGURE 3. (**A**) Examples of visual evoked potentials (VEPs) in response to gratings of different spatial frequency, and examples of the relative spatial resolution limit (**B**) by linear extrapolation to noise level (*dashed line*). (**C**) The averaged limit of cortical spatial resolution limit in the control mice (0.62 ± 0.01 cycle/deg, $n = 9$) was significantly higher than that in the adult α7 KO mice (0.42 ± 0.02 cycle/deg, $n = 7$; $^*P < 0.05$). (**D**) There were no differences between the VEP amplitude profiles of the WT and α7 KO mice in relation to the different electrodes positions along the mediolateral axis (the distance from lambda is shown on the *x*-axis) in terms of stimulation of the contralateral or ipsilateral eye. In (**A**), the vertical scale bar = 100 μV and the horizontal scale bar = 100 ms.

spatial resolution limit in each mouse was calculated by means of linear extrapolation of data points to the noise level, as shown in Figure 3B (VEP amplitudes were plotted as a function of spatial frequencies, semilog coordinates). The mean cortical spatial resolution limit in the control mice was 0.62 ± 0.01 cycle/deg ($n = 9$; Fig. 3C), which was similar to the value previously reported in the same mouse strain.[14] The spatial resolution limit was significantly reduced in the α7 KO mice (0.42 ± 0.02 cycle/deg, $n = 5$; $P < 0.05$ vs. controls; Fig. 3C), in line with the data obtained using Prusky's behavioral method[13] (see Figs. 2B, 2C).

To further explore cortical visual function, the contrast threshold was measured by recording the VEP responses to gratings at different contrasts (Fig. 4). VEP amplitude decreased with decreasing contrasts (from 90% to 0%). The amplitudes of the VEPs elicited by gratings of two different spatial frequencies (0.06 and 0.2 cycle/deg) were recorded as a function of the log contrast and the contrast threshold was calculated by means of the linear extrapolation of data to the noise level (Figs. 4A, 4B). The contrast thresholds at both spatial frequencies were not significantly different between the control mice (0.06 cycle/deg: contrast threshold = 5.2 ± 1%; 0.2 cycle/deg: contrast threshold = 15 ± 2%; $n = 9$; Fig. 4C) and the mutant mice (0.06 cycle/deg: contrast threshold = 4.4 ± 0.5%; 0.2 cycle/deg: contrast threshold = 17 ± 1%; $n = 5$; Fig. 4C). The lower cortical spatial resolution limit in α7 KO mice was therefore not dependent on the change in contrast gain.

To investigate the functional characteristics of the retina, we first used optical stimulator (Ganzfeld)–generated flashes in dark- and light-adaptation to record electroretinogram (F-ERG) responses in animals aged 2 to 3 months that had been reared under normal lighting conditions (12-hour light/12-hour dark cycle, maximum light intensity < 100 lux). The results clearly showed that there was no significant difference in the scotopic (at all light intensities) or light-adapted F-ERG (photopic) between the WT and α7 KO mice (Fig. 5).

Subsequently, we used PERG recordings to rule out the possibility that the reduced visual acuity of the α7 KO mice may have been due to altered retinal function. Pattern stimulation at 1-Hz reversal generated a transient retinal response that consisted of a smaller positive peak at approximately 90 ms, and a major negative component with peak latency at 150 ms (Fig. 6A). By measuring the peak-to-trough amplitude in response to increasing spatial frequencies we obtained an estimate of retinal spatial resolution limit (Fig. 6A) using a method previously described for VEPs. The retinal spatial resolution limit measured in the control mice (0.64 ± 0.03 cycle/deg, $n = 5$) was similar to the cortical spatial resolution limit determined by VEPs, and not statistically different from the retinal spatial resolution limit measured in the α7 KO mice (0.64 ± 0.02 cycle/deg, $n = 5$). This shows that the reduced visual acuity of α7 KO mice is not caused by an abnormal spatial resolution limit at the retinal level.

Data obtained from β2 KO mice show that their reduced visual acuity is due to an alteration in the segregation of retinofugal projections in the dorsolateral geniculate nucleus.[9] To rule out this possibility, we traced the retinogeniculate projections in control and α7 KO mice by means of the monocular intravitreal injection of fluorescent cholera toxin. The contralateral stained retinogeniculate terminals were distributed at the level of the "outer shell " of the dorsolateral geniculate nucleus (dLGN) located caudodorsally (Fig. 7A), and a labeling gap was visible in the dorsomedial part of the dLGN at the level of the "inner core, " a region that receives afferents

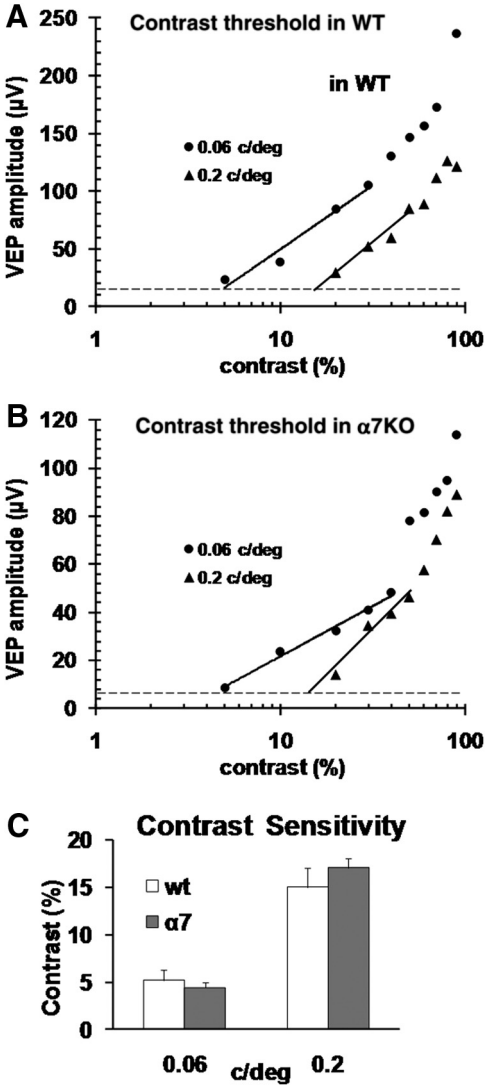

FIGURE 4. (**A**, **B**) Examples of contrast threshold calculations by means of the linear extrapolation to the noise level of VEPs (*dashed line*) in response to gratings at two different spatial frequencies (0.06 and 0.2 cycle/deg) in WT and α7KO mice. (**C**) The plot shows averaged cortical contrast sensitivity in WT ($n = 5$) and α7KO ($n = 5$) mice; there was no significant difference in mean contrast threshold between the WT and α7 KO mice ($P > 0.05$).

only from the ipsilateral retina. The ipsilateral labeled fibers not crossing at the level of the optic chiasm showed a complementary labeling pattern in the "inner core" of the ipsilateral dLGN (Fig. 7A). As shown in Figure 7A, the qualitative labeling of the contralateral and ipsilateral terminals in the dLGN was comparable in the control and α7 KO mice. The labeled retinal terminals were quantitatively evaluated by means of methods previously used by Rossi et al.,[9] which showed that there was no statistically significant difference in the percentage of the dLGN occupied by the ipsilateral fibers between the control mice (13.2 ± 0.1%, $n = 3$) and the α7 KO mice (12.8 ± 0.1%, $n = 3$) (Fig. 7B). The segregation of the retinofugal fibers is therefore normal in the LGN regions of α7 KO mice.

Finally, we evaluated the ocularity of α7 KO mice by recording the VEP responses elicited by the contralateral and ipsilateral eyes in the two cortices. The responses driven by the contralateral eye in the binocular portion of the visual cortex (OC1b, 2.8/3 mm from lambda) are larger than the responses elicited by ispilateral eye stimulation,[14] and this bias in favor of the contralateral eye reflects the predominance of crossed fibers at the chiasm and the distribution of LGN fibers. We measured the ratio between contralateral and ipsilateral response amplitudes in both OC1b regions, and considered it a cortical index of the balance between the inputs of the contralateral and ipsilateral eyes (ocularity). Because there was no significant difference between the α7 KO mice (3.1 ± 0.03, $n = 7$) and WT mice (2.8 ± 0.03, $n = 9$; Fig. 7C), the reduced visual acuity of the former is not associated with any alteration in the balance between the inputs of the two eyes (ocularity) in the primary visual cortex. In addition, we evaluated cortical retinotopy by measuring VEP amplitude profiles when the electrode was moved to different distances from lambda along the mediolateral axis (see Fig. 3D); cortical retinotopy using VEP closely corresponds to that previously reported by evaluating receptive field centers of single cortical units.[14] It is also worth noting that VEP retinotopy was normal in the α7 KO mice.

DISCUSSION

It has been reported that nAChRs (especially α7 nAChRs) are involved in differentiation, neuron migration, and synapse formation during brain development,[18–20] and the temporal pattern of nAChR expression suggests that they play a particular role because of their high concentration during the stage of synapse formation. The results of in vitro experiments indicate that nAChRs (particularly α7) may control the development of neuronal architecture, stabilize synapse formation, and orient and control neurite outgrowth.[18,19,21,22] Availability of mutant mice lacking individual nAChR subunits provides a unique opportunity to study their function in the nervous system.

Mice lacking the α7 nAChR subunit are viable and apparently normal in terms of their brain anatomy and performance of basic behavioral tasks, although they show some cognitive impairment in terms of episodic/working memory[5] and sus-

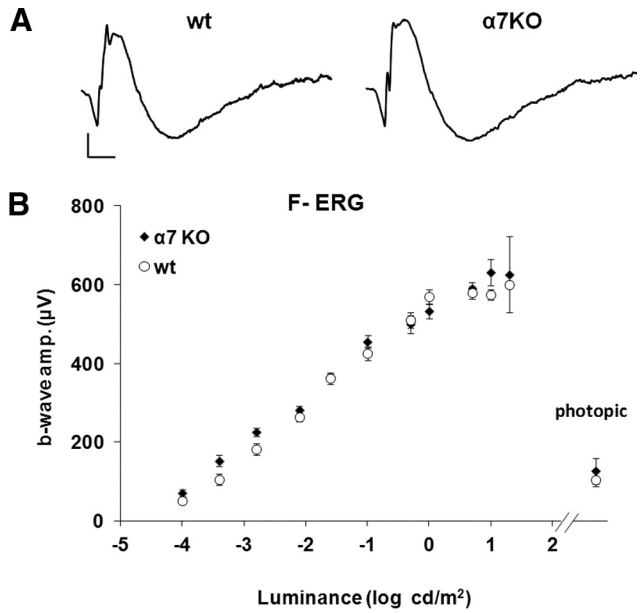

FIGURE 5. (**A**) Examples of scotopic F-ERG from WT (*left*) and α7KO mice (*right*) at the highest luminance intensity (20 cd s/m^2 × s^{-1}). (**B**) The mean F-ERG b-wave plotted as a function of increasing luminance (log cd/m^2) under scotopic conditions, and at 20 cd/m^2 in the presence of a constant background (15 cd/m^2, photopic conditions). In (**A**), the vertical scale bar = 200 μV and the horizontal scale bar = 100 ms.

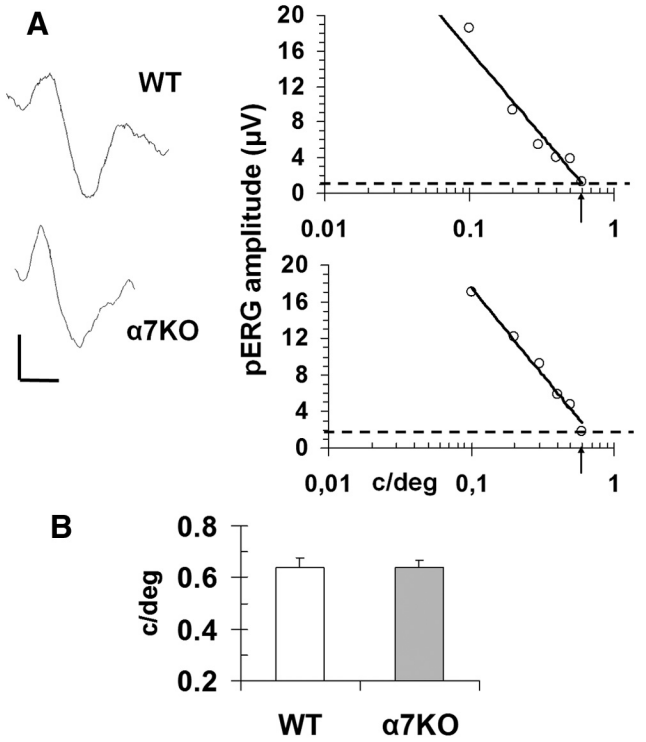

FIGURE 6. (**A**) Examples of PERG recordings from WT and α7KO mice at the spatial frequency of 0.06 cycle/deg; examples of the calculation of the retinal spatial resolution limit by means of linear extrapolation to noise level (*dashed line*) are shown on the *right*. (**B**) Mean spatial resolution was not significantly different between the WT (0.64 ± 0.03 cycle/deg, $n = 5$) and the α7KO mice (0.64 ± 0.02, $n = 3$). In (**A**), the vertical scale bar = 5 μV and the horizontal scale bar = 100 ms.

tained attention.[23,24] The fact that the absence of the α7 subunit has only a slight impact on behavioral performance suggests a possible compensatory effect in the nervous system. One recent study has found an increase in the number of α4- and α3-containing nAChRs in the cortex and hippocampus of α7 KO mice, which may contribute to normal brain development; however, these changes were limited to the first 21 days of postnatal development and there was no significant difference in subunit levels between adult α7 KO and WT mice.[25] Our binding and immunoprecipitation studies of 3-month-old mice confirmed that there is no significant difference in the levels of non-α7 subunits in the visual cortex and the retina of WT and α7 KO mice, thus excluding the possibility that the absence of the α7 subunit induces changes in the expression levels of the other nicotinic receptors.

Their good performance in basic tasks allowed us to determine behaviorally the visual acuity of α7 KO mice. They were able to learn the water maze task as quickly as the WT mice; however, despite the compensation provided by the other nicotinic receptor subunits during cortical development,[25] they were still visually impaired. Their reduced visual acuity when performing a behavioral task was confirmed by measurements of the cortical spatial resolution limit, which suggests that the α7 subunit plays a particular role in visual system development. It has been demonstrated that cholinergic neurotransmission through the nicotinic receptors on retinal ganglion cells is required for retinal wave generation,[26–28] and the refined formation of eye-specific layers at the thalamic level depends on retinal waves of spontaneous activity that are sensitive to nicotinic blockers in the P1–P10 time window.[29] Mice lacking the β2 subunit have altered retinal waves[29] and, consequently, abnormal retinofugal projections in the dorsolateral geniculate nucleus (dLGL) and superior colliculus that do not segregate into eye-specific areas; they are also affected by reduced visual acuity and altered cortical retinotopy.[9]

The α7 homomeric receptor is abundantly expressed in the neocortex, hippocampus, and subcortical limbic regions.[1] Concerning the visual pathways, the α7 subunit is expressed in the mouse retina with α-bungarotoxin labeling localized at terminals of amacrine cells on bipolar cells[30] as well as in the colliculus and in the dLGN.[1] Our PERG and F-ERG experiments excluded the possibility that the reduced visual acuity of adult α7 KO mice is due to abnormal retinal function. This is in line with previous findings showing that cortical but not retinal acuity is reduced in β2 KO mice,[9] and suggests that the lack of one specific nicotinic receptor subunit may affect visual system development but can be compensated by retinal function in adults. Moreover, unlike that of β2 KO mice, the reduced visual acuity of α7 KO mice is not due to an alteration in the segregation of retinal fibers, altered cortical retinotopy, or ocular dominance in the binocular region of the visual cortex. Previous studies have shown that both α4 and α7 mRNA levels in rodents accumulate from P12 before eye opening to about P35, with α7 subunit expression increasing in all cortical layers other than layer VI soon after eye opening. This indicates that visual cortex stimulation by a visual input is an essential step in normal α7 nAChR expression, and suggests that these receptors may play an experience-dependent role in visual cortex maturation.[8] Unlike other genetic manipulation,[31] synaptic changes in α7 KO mice reduce visual acuity without affecting

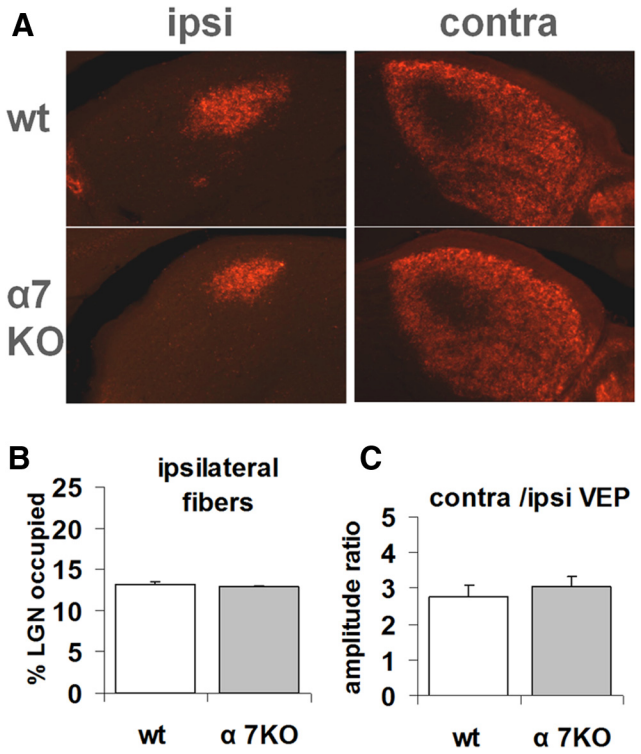

FIGURE 7. (**A**) Representative coronal sections of the contralateral and ipsilateral dLGNs (with respect to the injected eye) of WT and α7KO mice. Labeling by means of an intraocular injection of fluorescently tagged cholera toxin B subunit showed that the α7KO mice have normal retinogeniculate projections. (**B**) There was no difference in the percentage dLGN area occupied by ipsilateral fibers between the WT (13.2 ± 0.1%, $n = 3$) and α7KO mice (12.8 ± 0.1%, $n = 3$). (**C**) There was also no significant difference in the ratio of contralateral and ipsilateral VEP amplitude responses (KO, 3.1 ± 0.03, $n = 7$ vs. WT, 2.8 ± 0.03, $n = 9$).

contrast sensitivity, thus suggesting that the decreased response to high spatial frequencies may be due to an altered cortical receptive field or unbalanced excitation/inhibition at cortical synapses. One possibility is that the lack of α7 receptors at cortical synapses affects the release of other presynaptic neurotransmitters or alters calcium permeability pre- and postsynaptically. It has been clearly shown that α7 nAChRs represent a highly calcium-permeable channel that enhances calcium influx by modulating the release of neurotransmitters such as glutamate and γ-aminobutyric acid[32–34]; in particular, homomeric α7 nAChRs boost the release of glutamate, thus facilitating the induction of long-term synaptic potentiation (LTP). Although the specific role of nicotinic receptors in visual cortex synaptic plasticity still needs to be thoroughly investigated, there is evidence that cholinergic system activity is involved in the plastic reorganization of neuronal connectivity in the cerebral cortex.[8] Moreover, both LTP and long-term depression, two forms of synaptic plasticity that are thought to participate in the shaping of neuronal connections as well as learning and memory, are regulated by cholinergic transmission.[35–38] It therefore cannot be excluded that the cortical deficit in α7 KO mice may lead to the abnormal functional development of cortical circuitry as a result of defective synaptic plasticity.

Our findings show that the presence of the α7 subunit during embryogenesis is not crucial for prenatal brain development, including visual system formation, but indicate that the homomeric α7 receptor plays a critical role in visual cortex refinement and functional maturation. It is worth noting that patients with homozygous or compound heterozygous deletions in 15q13.3 involving several genes (including *Chrna7* deletions) develop neurodevelopmental disorders with severe encephalopathy, hypotonia, and visual impairment[39]; our findings show that mice with a homozygous deletion of the gene for the α7 subunit (mice that are homozygous for the *Chrna7*^{tm1Bay} mutation) are affected by a visual cortical dysfunction that leads to poor vision.

Acknowledgments

The authors thank Matteo Caleo (Neuroscience Institute, Pisa, Italy) for his helpful discussions and suggestions, Enrico Cherubini (SISSA, Trieste, Italy) for his help with the studies of α7 KO mice, Giulio Cappagli and Carlo Orsini for the online acquisition software and their technical assistance, and Kevin Smart (native English speaker) who revised the manuscript.

References

1. Gotti C, Clementi F. Neuronal nicotinic receptors: from structure to pathology. *Prog Neurobiol.* 2004;74:363–396.
2. Orr-Urtreger A, Goldner FM, Saeki M, et al. Mice deficient in the alpha7 neuronal nicotinic acetylcholine receptor lack alpha-bungarotoxin binding sites and hippocampal fast nicotinic currents. *J Neurosci.* 1997;17:9165–9171.
3. Paylor R, Nguyen M, Crawley JN, Patrick J, Beaudet A, Orr-Urtreger A. Alpha7 nicotinic receptor subunits are not necessary for hippocampal-dependent learning or sensorimotor gating: a behavioral characterization of Acra7-deficient mice. *Learn Mem.* 1998;5:302–316.
4. Marubio LM, Paylor R. Impaired passive avoidance learning in mice lacking central neuronal nicotinic acetylcholine receptors. *Neuroscience.* 2004;129:575–582.
5. Fernandes C, Hoyle E, Dempster E, Schalkwyk LC, Collier DA. Performance deficit of alpha7 nicotinic receptor knockout mice in a delayed matching-to-place task suggests a mild impairment of working/episodic-like memory. *Genes Brain Behav.* 2006;5:433–440.
6. Levin ED, Bradley A, Addy N, Sigurani N. Hippocampal alpha 7 and alpha 4 beta 2 nicotinic receptors and working memory. *Neuroscience.* 2002;109:757–765.
7. Gotti C, Moretti M, Gaimarri A, Zanardi A, Clementi F, Zoli M. Heterogeneity and complexity of native brain nicotinic receptors. *Biochem Pharmacol.* 2007;74:1102–1111.
8. Aztiria E, Gotti C, Domenici L. Alpha7 but not alpha4 AChR subunit expression is regulated by light in developing primary visual cortex. *J Comp Neurol.* 2004;480:378–391.
9. Rossi FM, Pizzorusso T, Porciatti V, Marubio LM, Maffei L, Changeux JP. Requirement of the nicotinic acetylcholine receptor beta 2 subunit for the anatomical and functional development of the visual system. *Proc Natl Acad Sci USA.* 2001;98:6453–6458.
10. Champtiaux N, Changeux JP. Knock-out and knock-in mice to investigate the role of nicotinic receptors in the central nervous system. *Curr Drug Targets CNS Neurol Disord.* 2002;1:319–330.
11. Grady SR, Moretti M, Zoli M, et al. Rodent habenulo-interpeduncular pathway expresses a large variety of uncommon nAChR subtypes, but only the alpha3beta4* and alpha3beta3beta4* subtypes mediate acetylcholine release. *J Neurosci.* 2009;29:2272–2282.
12. Moretti M, Mugnaini M, Tessari M, et al. A comparative study of the effects of the intravenous self-administration or subcutaneous minipump infusion of nicotine on the expression of brain neuronal nicotinic receptor subtypes. *Mol Pharmacol.* 2010;78:287–296.
13. Prusky GT, West PW, Douglas RM. Behavioral assessment of visual acuity in mice and rats. *Vision Res.* 2000;40:2201–2209.
14. Porciatti V, Pizzorusso T, Maffei L. The visual physiology of the wild type mouse determined with pattern VEPs. *Vision Res.* 1999;39:3071–3081.
15. Porciatti V. The mouse pattern electroretinogram. *Doc Ophthalmol.* 2007;115:145–153.
16. Porciatti V, Saleh M, Nagaraju M. The pattern electroretinogram as a tool to monitor progressive retinal ganglion cell dysfunction in the DBA/2J mouse model of glaucoma. *Invest Ophthalmol Vis Sci.* 2007;48:745–751.
17. Moretti M, Vailati S, Zoli M, et al. Nicotinic acetylcholine receptor subtypes expression during rat retina development and their regulation by visual experience. *Mol Pharmacol.* 2004;66:85–96.
18. Lipton SA, Kater SB. Neurotransmitter regulation of neuronal outgrowth, plasticity and survival. *Trends Neurosci.* 1989;12:265–270.
19. Role LW, Berg DK. Nicotinic receptors in the development and modulation of CNS synapses. *Neuron.* 1996;16:1077–1085.
20. Coronas V, Durand M, Chabot JG, Jourdan F, Quirion R. Acetylcholine induces neuritic outgrowth in rat primary olfactory bulb cultures. *Neuroscience.* 2000;98:213–219.
21. Pugh PC, Berg DK. Neuronal acetylcholine receptors that bind alpha-bungarotoxin mediate neurite retraction in a calcium-dependent manner. *J Neurosci.* 1994;14:889–896.
22. Zheng JQ, Felder M, Connor JA, Poo MM. Turning of nerve growth cones induced by neurotransmitters. *Nature.* 1994;368:140–144.
23. Young JW, Finlayson K, Spratt C, et al. Nicotine improves sustained attention in mice: evidence for involvement of the alpha7 nicotinic acetylcholine receptor. *Neuropsychopharmacology.* 2004;29:891–900.
24. Young JW, Crawford N, Kelly JS, et al. Impaired attention is central to the cognitive deficits observed in alpha 7 deficient mice. *Eur Neuropsychopharmacol.* 2007;17:145–155.
25. Yu WF, Guan ZZ, Nordberg A. Postnatal upregulation of alpha4 and alpha3 nicotinic receptor subunits in the brain of alpha7 nicotinic receptor-deficient mice. *Neuroscience.* 2007;146:1618–1628.
26. Feller MB, Wellis DP, Stellwagen D, Werblin FS, Shatz CJ. Requirement for cholinergic synaptic transmission in the propagation of spontaneous retinal waves. *Science.* 1996;272:1182–1187.
27. Penn AA, Riquelme PA, Feller MB, Shatz CJ. Competition in retinogeniculate patterning driven by spontaneous activity. *Science.* 1998;279:2108–2112.
28. Sernagor E, Eglen SJ, O'Donovan MJ. Differential effects of acetylcholine and glutamate blockade on the spatiotemporal dynamics of retinal waves. *J Neurosci.* 2000;20:RC56(1–6).
29. Bansal A, Singer JH, Hwang BJ, Xu W, Beaudet A, Feller MB. Mice lacking specific nicotinic acetylcholine receptor subunits exhibit dramatically altered spontaneous activity patterns and reveal a

limited role for retinal waves in forming ON and OFF circuits in the inner retina. *J Neurosci.* 2000;20:7672–7681.

30. Pourcho RG. Localization of cholinergic synapses in mammalian retina with peroxidase-conjugated alpha-bungarotoxin. *Vision Res.* 1979;19:287–292.
31. Heimel JA, Saiepour MH, Chakravarthy S, Hermans JM, Levelt CN. Contrast gain control and cortical TrkB signaling shape visual acuity. *Nat Neurosci.* 2010;13:642–648.
32. Alkondon M, Pereira EF, Albuquerque EX. Mapping the location of functional nicotinic and gamma-aminobutyric acid A receptors on hippocampal neurons. *J Pharmacol Exp Ther.* 1996;279:1491–1506.
33. Alkondon M, Rocha ES, Maelicke A, Albuquerque EX. Diversity of nicotinic acetylcholine receptors in rat brain. V. alpha-Bungarotoxin-sensitive nicotinic receptors in olfactory bulb neurons and presynaptic modulation of glutamate release. *J Pharmacol Exp Ther.* 1996;278:1460–1471.
34. MacDermott AB, Role LW, Siegelbaum SA. Presynaptic ionotropic receptors and the control of transmitter release. *Annu Rev Neurosci.* 1999;22:443–485.
35. Brocher S, Artola A, Singer W. Agonists of cholinergic and noradrenergic receptors facilitate synergistically the induction of long-term potentiation in slices of rat visual cortex. *Brain Res.* 1992;573:27–36.
36. Kirkwood A, Rozas C, Kirkwood J, Perez F, Bear MF. Modulation of long-term synaptic depression in visual cortex by acetylcholine and norepinephrine. *J Neurosci.* 1999;19:1599–1609.
37. Pesavento E, Margotti E, Righi M, Cattaneo A, Domenici L. Blocking the NGF-TrkA interaction rescues the developmental loss of LTP in the rat visual cortex: role of the cholinergic system. *Neuron.* 2000;25:165–175.
38. Origlia N, Kuczewski N, Aztiria E, Gautam D, Wess J, Domenici L. Muscarinic acetylcholine receptor knockout mice show distinct synaptic plasticity impairments in the visual cortex. *J Physiol.* 2006;577:829–840.
39. Lepichon JB, Bittel DC, Graf WD, Yu S. A 15q13.3 homozygous microdeletion associated with a severe neurodevelopmental disorder suggests putative functions of the TRPM1, CHRNA7, and other homozygously deleted genes. *Am J Med Genet A.* 2010;152A:1300–1304.